The Effect of Neck Stiffness on the Response of a Surrogate Head due to Blunt Trauma in Judo

Jon Farmer, Séan Mitchell, Paul Sherratt and Yusuke Miyazaki

Abstract Acute subdural hematomas can result from blunt trauma due to unbraced backwards falls in judo. This study investigated the response of a surrogate head subjected to blunt trauma from experimental backwards falls. The head was constrained by a Hybrid III surrogate neck (stiff condition) and by a novel surrogate neck (less stiff condition) attached to a simplified surrogate torso. A DTS 6DX Pro sensor was used to record linear acceleration and angular rate data and has been reported at the head's centre of gravity. Peak angular acceleration values of ~9600 - 11000 rad/s^2 and ~1500 - 1800 rad/s^2 were recorded for the novel surrogate neck and the Hybrid III surrogate neck, respectively. The novel surrogate neck predicted acute subdural haematomas through bridging vein rupture when considering threshold values. The study indicates that angular kinematics of the head in the sagittal plane could be significantly underestimated when constrained by an overly stiff surrogate neck, such as the Hybrid III surrogate neck.

Keywords Acute subdural hematoma, blunt trauma, surrogate neck, traumatic brain injury.

I. INTRODUCTION

Acute subdural hematoma (ASDH) is a traumatic brain injury (TBI) with high mortality rates within sports [1]. Combat sports such as judo introduce interactions whereby participants are thrown to a stiff practice mat and are required to perform techniques such as the *backwards break fall* (Figure 1) to safely fall to the mat. If performed incorrectly, i.e., with unbraced neck musculature, this technique can have catastrophic consequences. Between 2003 and 2010, Japanese judo reported 30 head injury cases due to blunt trauma of the skull with the mat, following a backwards fall. In 28 of the 30 cases, ASDH was diagnosed due to the rupturing of parasagittal bridging veins and 15 of these injuries were fatal [2]. These injury statistics show that the inexperienced participants had an increased injury rate compared to the experienced participants.

Incorrect execution of the break fall involves limited use of the arms and extension of the neck that results in blunt trauma between the occipital region of the skull and the mat. Two kinematic studies of human volunteers showed that lower neck extension momentum [3] and greater utilisation of hand-to-ground contact resulted in decelerated head motion [4] in experienced participants, when compared to novices. However, due to ethical constraints, neither study was able to show kinematics of an injurious impact. Controlled and simplified laboratory experiments, representing the backwards break fall of the judo participants, could offer valuable insight into the mechanism of injury. The use of Anthropomorphic Test Devices (ATDs) or mechanical surrogates that represent all, or regions of the human, i.e., head and neck, provide an ethical and repeatable alternative to the human volunteer.

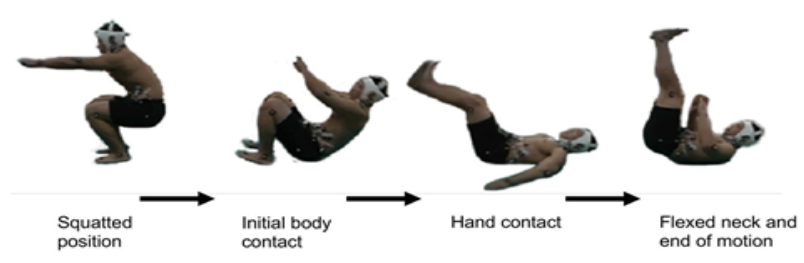

Fig. 1. Visual representation of the correct backwards break fall technique (adapted from [4]).

J. Farmer is a Research Associate, S. Mitchell and P. Sherratt are Senior Lecturers at the Sports Technology Institute, Loughborough University, United Kingdom (j.farmer@lboro.ac.uk, +44 1509 564827). Y. Miyazaki is an Associate Professor at the Tokyo Institute of Technology, Japan.

However, the surrogate is only valid if it behaves in a similar manner to the human under equivalent test conditions. Importantly, the response of the human head during and after an impact can be significantly affected by the properties of the neck: the head trajectory is strongly influenced by the more rigid elements of the neck whereas rapid acceleration may be permitted by the more flexible elements. Therefore, the aim of this research was to investigate whether the constraint imposed by a surrogate neck, significantly affects the response of an instrumented surrogate head, when subjected to backwards falls commonly seen in judo.

II. METHODS

Surrogate Selection

Given the mainly sagittal motion of the backwards break fall technique and the almost exclusive use of the commercially available Hybrid III surrogate neck (H3SN) in other sport-related head injury research, the H3SN (Figure 2a) was chosen as the primary surrogate neck for the investigation. The neck was designed for the purpose of frontal car collisions with a sagittal plane neck stiffness response influenced by biomechanical corridors specified by braced human neck data [5]. The sagittal plane bending stiffness of the H3SN is reportedly 10 times stiffer than the typical human neck in passive unbraced sagittal flexion and extension [6-8].

The novel surrogate neck (NSN) (Figure 2b) was designed to be comparable to the H3SN and was based on the computational simulations of [7], whose results showed that the response of the H3SN could be closely approximated by a single link with two pivots. The NSN was therefore constructed as a single link, pin-jointed mechanism with motion limited to the sagittal plane. The joint centres were matched to the upper and lower H3SN joint centres. These locations, along with reference of a Frankfort horizontal plane in the surrogate head model, provided the neutral posture and ensured matched placement of the surrogate head to the H3SN. The NSN has a total ROM of 120°, which is comparable to the H3SN and the mean reported ROM of the human cervical spine from *in vivo* radiographic studies [9-11]. The human data also suggests that the ROM is distributed across the upper and lower cervical spine in a ratio of 1:2, respectively. The NSN ROM was therefore distributed as 40° and 80° between the upper and lower joints, respectively. The resistance to motion at the two joints was deliberately minimal, i.e. inertial resistance only, to provide an evaluation of two extreme conditions. The inertial properties of the NSN were matched to those of the H3SN and finally, the NSN was designed to be compatible with an advanced surrogate head model [12] and a judo surrogate torso [13].

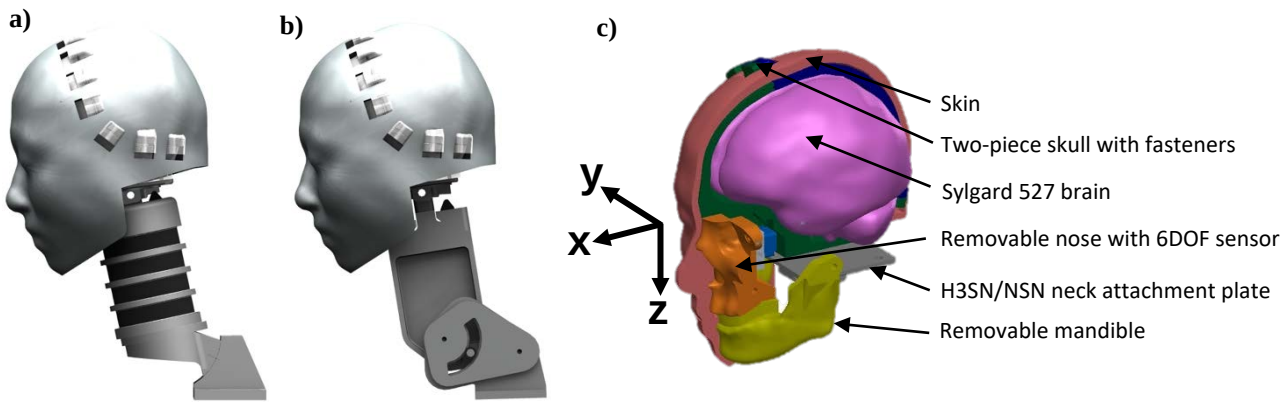

Fig. 2a). The H3SN with surrogate head attached. b) The NSN with surrogate head attached. c) Section view and key features of the novel surrogate head.

The novel surrogate head (Figure 2c), used throughout, was identical to that used by [12] and a 6DOF sensor (DTS 6DX Pro) was affixed to the removable polycarbonate nose to measure the response of the skull. A judo surrogate torso [13] representing a squatted backwards break fall technique was used for the study. The surrogate was matched to average characteristics of junior high school judo participants (mass: 44.5 kg, height (squatted): 1.03 m and centre of gravity (COG): 0.462 m).

Other Equipment

A schematic representation of the experimental setup can be seen in Figure 3. The trials were conducted on an International Judo Federation (IJF) approved Tatami judo mat. The shoulder region of the judo surrogate was raised to 70° from the horizontal to achieve an impact velocity of 3.5 m/s, matching kinematic data of actual judo participants performing the backwards fall when thrown by the Osoti-gari technique [13]. A lightweight nylon, spring-loaded mechanism was used to maintain the neutral alignment of the NSN during the fall phase of the surrogate and post-analysis of high-speed video images were conducted to ensure that the release mechanism was in place at the time of torso impact, confirming matched alignment of the NSN and H3SN. The mechanism was designed to release from the surrogate neck prior to head impact, ensuring that the head-neck complex could naturally rotate and translate due to the inertial loading. A total of 10 trials were recorded, five for each of the neck conditions.

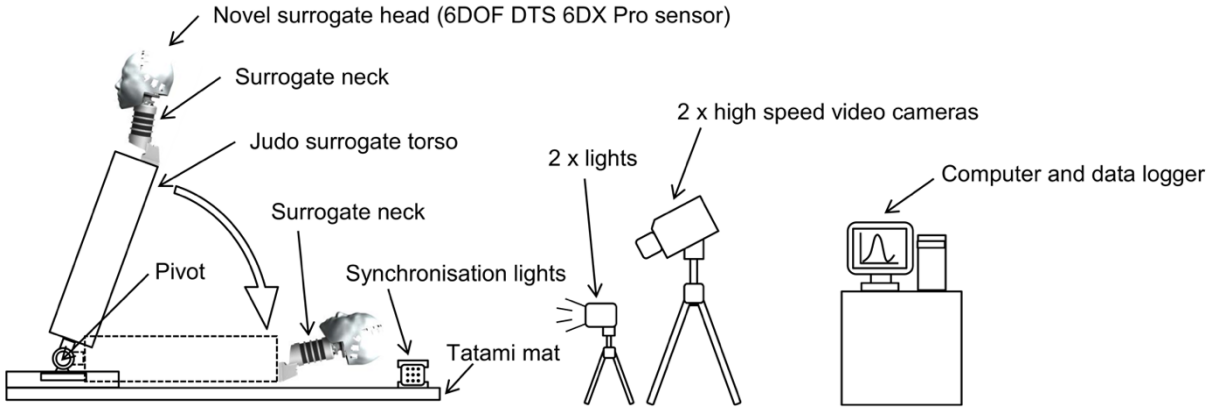

Fig. 3. Schematic representation of the test equipment and setup.

Data Capture and Processing

A calibrated DTS 6DX Pro sensor (3DOF accelerometer and 3DOF gyroscope) was used to record triaxial linear acceleration and angular velocity data to a data logger (DCS100A) at a sampling rate of 10 kHz. The raw angular velocity and linear acceleration data were processed using a bespoke MATLAB script. The frequency content of the raw signal was investigated using frequency spectral analysis and residual analysis. A low pass, fourth order Butterworth filter with a cut off frequency of 80 Hz was applied to the raw data which had negligible effect on the dominant shape and magnitude of the resulting curves but enabled a clear qualitative description of the skull kinematics to be made and compared between the two neck conditions. The first cycle of the motion was included for analysis and comprised the initial fall from start position, the shoulder and subsequent head contact with the mat and the resulting flexion and translational motion of the head/neck/torso complex away from the mat. The resulting skull kinematics are presented in accordance with the SAE J211 recommended local coordinate system, as shown in Fig.2c.

To quantify the differences in linear and angular responses due to the constraint of the surrogate necks, impact metrics such as peak linear acceleration (PLA), peak angular acceleration and peak angular velocity are reported in the results. In addition, calculated metrics such as peak to peak change in angular velocity (PPCAV) are also reported. Peak angular velocity has been strongly correlated with strain in bridging veins (BVs) when modelling ASDH through bridging vein rupture (BVR) [14]. Further to this, PPCAV has been shown to correlate well with brain surface displacement through experimental and computational modelling of frontal sled collisions [12]. The risk of sustaining ASDH has also been predicted with threshold values for BVR [15]. In the previous research, Post-Mortem Human Subject (PMHS) experiments were conducted on 19 full body specimens positioned in a seated, upright posture and impacted with a pendulum to the back of the head. Angular acceleration pulses were reported along with their corresponding impact durations and have been adapted in this research to present a BVR threshold curve for the impacts. Finally, SPSS statistical software (IBM, 2015) was used to investigate differences between the H3SN and the NSN. Statistical differences, where reported, have been found with significance $P < 0.05$.

III. RESULTS

Qualitative Impact Behaviour of the Surrogate Head

The typical response of the head when constrained by the H3SN (Figure 4a and 4b) was initiated by ground contact at the shoulder region of the surrogate (1) resulting in translation of the head towards the mat (2). The subsequent increase in positive linear and angular acceleration of the head at (3), results from an impact location above the head's COG. The linear acceleration then developed on to the lower region of the head, below the COG, to a maximum positive value at (4). The head contact with the mat acted to reverse the direction of the angular acceleration and thus resulted in a negative angular acceleration and a rising of the mandible bone as the head/neck/torso complex left the mat at (5). Finally, the neck is seen to enter a mode of flexion as the complex continues to rise vertically away from the mat at (6). The typical response of the head when constrained by the NSN (Figure 4c and 4d) was initiated by the ground contact at the shoulder region of the surrogate (7), resulting in an inertial effect at the lower neck pivot (8). The lower region of the surrogate head then contacted the mat (9) causing a positive linear acceleration and negative angular acceleration of the head. The head proceeded with a rolling motion along the mat changing the centre of pressure (CoP), above the COG, whilst the linear acceleration reached a maximum positive value (10). The change in CoP acted to reverse the direction of the angular acceleration and thus resulted in a positive angular acceleration. A rapid decrease in linear acceleration followed as the head left the ground (11) and the neck became flexed.

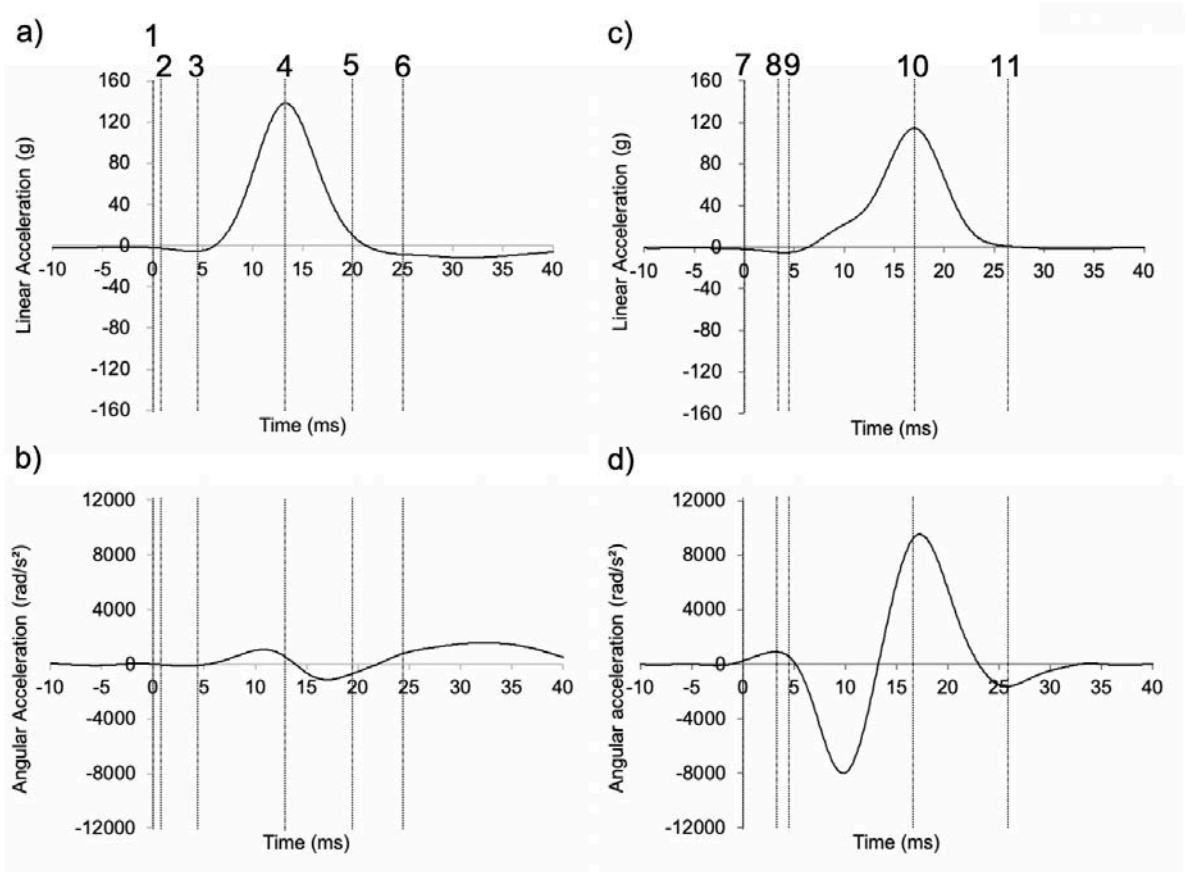

Fig. 4. Time history curves of the surrogate head: a) Linear acceleration of the H3SN; b) Angular acceleration of the H3SN; c) Linear acceleration of the NSN; d) Angular acceleration of the NSN.

Quantitative Impact Behaviour of the Surrogate Head

The calculated mean (± one standard deviation) peak values are presented in Table 1. Statistically significant differences were found for all impact metrics between the H3SN and the NSN conditions. The PLA and linear impulse (LI) decreased, whilst the impact duration (ID) was shown to increase for the NSN compared to the H3SN. The differences in angular kinematics were more substantial and the NSN displayed greater magnitudes of all measured and calculated metrics. The magnitudes of peak positive and negative angular accelerations were up to 9479 rad/s^2 and 6548 rad/s^2 greater, respectively. The NSN resulted in a calculated value of PPCAV of approximately three times that of the H3SN.

TABLE 1
MEAN (± STANDARD DEVIATION) IMPACT PHENOMENA

Neck Condition	PLA[1] (g)	ID[2] (ms)	LI[3] (N.s)	PPAA[4] (rad/s²)	PNAA[5] (rad/s²)	PPAV[6] (rad/s)	PNAV[7] (rad/s)	PPCAV[8] (rad/s)	PCAI[9] (Nm.s)
H3SN	136.2 (2.4)	13.3 (0.1)	3.9 (0.0)	1625 (120)	(-) 1352 (214.0)	14.0 (0.9)	(-) 6.6 (0.2)	20.6 (1.0)	0.1 (0.0)
NSN	110.7 (2.0)*	19.3 (0.8)*	3.4 (0.1)*	10555 (557.2)*	(-) 7459 (245.7)*	16.7 (1.5)*	(-) 45.8 (1.6)*	62.5 (2.7)*	3.7 (0.1)*

[1]Peak resultant liner acceleration [2]Impact duration [3]Linear impulse [4]Peak positive angular acceleration [5]Peak negative angular acceleration [6]Peak positive angular velocity [7]Peak negative angular velocity [8]Peak to peak change in angular velocity [9]Peak change in angular impulse [*]Statistically significant difference

The recorded impact durations of the H3SN and NSN of 13.2 ms - 13.4 ms and 18.5 ms - 20.3 ms, respectively, were calculated to correspond to peak angular acceleration threshold values of 7193 rad/s^2 - 7127 rad/s^2 and 5852 rad/s^2 - 5529 rad/s^2 for likely BVR [15-16]. Figure 5 presents the peak angular acceleration values versus impact duration values for each neck condition, along with the predicted BVR threshold curve. The NSN can be seen to exceed its respective threshold whilst the H3SN presents a very low risk of predicted BVR.

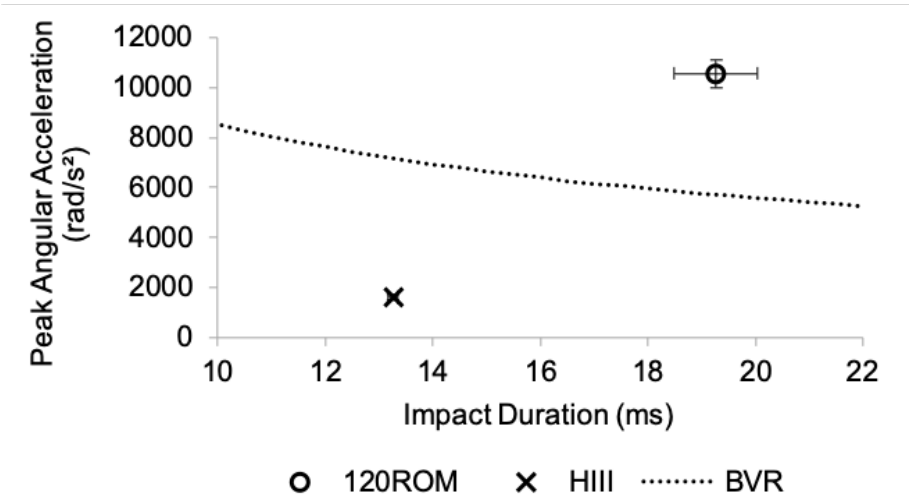

Fig. 5. Peak angular acceleration and impact duration with a predicted BVR threshold curve, as adapted from [15-16].

IV. DISCUSSION

The main aim of this research was to investigate the effect of neck stiffness on the measurable impact phenomena experienced by a surrogate head due to backwards falls. The less constrained design of the NSN resulted in a decrease in peak linear acceleration and linear impulse and an increase in impact duration. The neck constraint influenced the head's impact location following the inertial loading at the shoulder region and this had a significant effect on the kinematics of the head during the impact. The impact location on the head below and above the COG for the NSN and H3SN, respectively, led to a large negative angular acceleration in the case of the NSN. The H3SN provided a much higher resistance to motion than the NSN, which combined with the short duration over which the acceleration could act, reduced the peak negative angular velocity by up to six times. The angular kinematics (acceleration and velocity) were found to be the phenomena most affected by the constraint and greater differences were found between the H3SN and the NSN for peak negative angular velocity compared to peak positive angular velocity.

Whilst specific injury criterions for ASDH are limited, the recorded peak angular acceleration values and impact duration results were compared to values predicted to result in BVR from PMHS studies [15-16]. The H3SN results suggested that the peak angular acceleration values were insufficient to cause BVR, whilst the NSN significantly exceeded their respective threshold values. The BVR curve was based on reported PMHS data and whilst the bridging veins (BVs) are unlikely to be significantly different postmortem due to being fibrous and not containing muscle tissue, the data is not without limitations. Namely, the number and placement of BVs are specific to the individual and so it is unclear how those individuals injured during the break fall technique would compare to those used in the PMHS studies. Furthermore, limitations in the design of the NSN (i.e. inertial resistance only and single plane of motion) are not fully representative of the human neck and likely overestimate the peak values typically experienced by the human head during a backwards fall. However, the NSN does demonstrate that a surrogate neck with less bending stiffness than the H3SN can result in increased head angular motion, which potentially explains the occurrence of ASDH through exceeding BVR thresholds.

V. CONCLUSIONS

The research presents the evaluation of an initial surrogate neck design and directly compares its response to the H3SN. The NSN appears to offer a low cost, highly repeatable alternative to the H3SN, and in some regards, reveals findings that would otherwise be masked by the overly stiff H3SN. Specifically, the judo break fall impact scenario highlights the potential to underestimate angular kinematics of an unbraced surrogate head when the sagittal plane is overly constrained by a stiff surrogate neck. This underestimation is significant when investigating TBIs such as ASDH, whose prediction is highly correlated to angular kinematics. The comparison between the outcomes of the H3SN and NSN is perhaps similar to the comparison between skilled (braced) break fall participants and unskilled (unbraced) beginners. The latter gives rise to higher risk of BVR and potentially explains the increased injury rate observed in the sport. To explore means beyond the correct break fall technique to mitigate injuries in the less skilled, surrogate components that simulate vulnerable (beginners) are needed in addition to those that simulate the skilled individuals. The investigation is not without limitations and notably, the NSN is constrained to pivot at two joints within the ROM of a single plane. The NSN and H3SN neck stiffnesses present two extreme conditions and both are likely to over and underestimate the angular kinematics of the skull, respectively.

VI. ACKNOWLEDGEMENT

We would like to thank Stephen Carr from the Sports Technology Institute for manufacturing the novel surrogate neck. We would also like to thank the Japan Society for the Promotion of Science (JSPS) for selecting Jon Farmer to be a JSPS Summer Program Research Fellow.

VII. REFERENCES

[1] Fernandes, F.A.O and Sousa, R.J.A. (2015). Head injury predictors in sports trauma – a state of the art review. Journal of engineering in medicine, 229 (8): pp.592-608.
[2] Kamitani, T; Nimura, Y; Nagahiro, S; Miyazaki, S. and Tomatsu, T. (2013). Catastrophic head and neck injuries in judo players in japan from 2003 to 2010. American journal of sports medicine, 41 (8): pp.1915-1921.
[3] Koshida, S; Ishii, T; Matsuda, T. and Hashimoto, T. (2016). Kinematics of judo break fall for osoto-gari: considerations for head injury prevention. Journal of sports science, 35 (11): pp.1059-1065.
[4] Koshida, S; Ishii, T; Matsuda, T. and Hashimoto, T. (2014). Biomechanics of the judo backwards break fall: comparison between experienced and novice judokas. *Archives of Budo*, 187 (10): pp.188-194.
[5] Mertz, H.J. and Patrick, L.M. (1971). Strength and response of the human neck. *SAE transactions*, 80 (4): pp.2903-2928.
[6] Cappon, H.J; Philippens, M.M.G.M; Van Ratingen, M.R. and Wismans, J.S.H.M. (2000). Evaluation of dummy behavior during low severity rear impact. *Proceedings of IRCOBI conference*, 2000, Bron, France.
[7] Doherty, B.J. and Paver, J.G. (1988). Mathematical modelling of the Hybrid III manikin head-neck structure. Mathematical and computer modelling, 11: pp.430-435.

[8] Friedman, D; Paver, J.G. and Carlin, F. (2009). Hybrid III correlation with human injury potential in rollovers. *Proceedings of the ASME summer bioengineering conference*, 2009, Lake Tahoe, CA, USA.
[9] Siegler, S; Caravaggi, P; Tangorra, J; Milone, J; Namani, R. and Marchetto, P.A. (2015). The envelope of motion of the cervical spine and its influence on the maximum torque generating capability of the neck muscles. Journal of biomechanics, 48: pp.3650-3655.
[10] Shen, Q. and He, X. (2014). Bivariate analysis of cervical spine extension-neutral- flexion movements. Advances in biomedical science and engineering, 1: pp.33-44.
[11] Strimpakos, N; Sakellari, V; Gioftsos, G; Papathanasiou, M; Brountzos, E; Kelekis, D; Kapreli, E. and Oldham, J. (2005). Cervical spine ROM measurements: optimizing the testing protocol by using a 3D ultrasound-based motion analysis system. Cephalalgia, 25: pp.1133-1145.
[12] Miyazaki, Y; Railkar, A; Awamori, S; Kokeguchi, A; Amamori, I; Katagiri, M. and Yoshii, K. (2017). Intracranial brain motion measurement in frontal sled tests by using a new anthropometric test dummy head capable of direction brain motion evaluation and visualisation. *Proceeding of IRCOBI conference*, 2017, Antwerp, Belgium.
[13] Aiba, K; Omiya, M; Iteya, M; Kamitani, T. and Tomatsu, T. (2012). Comparison of evaluation indices for acute subdural hematoma occurrence under occipital impacts and effectiveness of head protectors in judo. Transactions of the Japan society of mechanical engineers, 78 (796): pp.1631-1641.
[14] Cui, Y.Z; Famaey, N; Depreitere, B; Ivens, J; Kleiven, S. and Sloten, J.V. (2016). On the assessment of bridging vein rupture associated acute subdural hematoma through finite element analysis. Computer methods in biomechanics and biomedical engineering, 20(5): pp.530-539.
[15] Depreitere, B; Lierde, C.V; Sloten, J.V; Audekercke, R.V; Perre, G.VD. Plets, C. et al. (2006). Mechanics of acute subdural hematomas resulting from bridging vein rupture. Journal of neurosurgery, 104: pp.950-956.
[16] Löwenhielm, P. Dynamic properties of the parasagittal bridging veins. (1974). *Zeitschrift für Rechtsmedizin* (journal of legal medicine), 74: pp.55–62.